ISSN: 0886-9685

Predrilled Holes for Pile Support of Skewed Integral Abutment Bridges

Andreas Parachos[1], and Amde Amde[2]

[1] Engineering, New York City College, NYC
[2] Civil Engineering, University of Maryland, College Park

E-mail: andreas_paraschos@yahoo.com

Received 09/08/2020
Accepted for publication 11/18/2020
Published 11/21/2020

Abstract

Integral abutment bridges, despite their limitations, represent the preferred option of state transportation agencies for both new and replacement bridges. This is due to their advantages over conventional bridges, including construction and maintenance cost savings. Bridge length is one of most notable limitations of integral abutment bridges. This is attributed to the fact that longer integral abutment bridges cause high bending stresses in the piles supporting integral abutments. Consequently, finding a way to reduce pile stresses may allow construction of longer integral bridges. Predrilled oversize holes of adequate depth filled with loose sand after pile driving is one of the most effective methods to reduce pile bending stresses. This paper investigates the relation between depth of predrilled holes and reduction in pile bending stresses. Analysis results confirm the reduction in pile bending stresses as a result of predrilling holes of adequate depth filled with loose sand and effective depth for predrilled holes is discussed.

Keywords: Bridges, steel; Bridge abutments; Bridges, skew; Steel piles; Soil properties; Finite element method

1. Introduction

Integral abutment bridges are girder bridges with no expansion joints in the bridge deck and no bearings at the abutments. The ends of girders are integral with the abutments. During thermal expansion and contraction, the superstructure and abutments move together into and away from the backfill.

Integral abutment bridges have been used for decades in the United States. A testament of their excellent performance over the years is the fact that the current policy of the vast majority of states is to build integral abutment bridges whenever possible. Although the use of integral abutment bridges offers numerous advantages over conventional bridges, there are limitations on their use. This is attributed to three reasons: (1) relatively limited research has been conducted on integral abutment bridges, (2) nationally-accepted design specifications for integral abutment bridges do not exist, and (3) there has been very little verification of the behavior of integral abutment bridges or direct evaluation of the validity of design assumptions through field monitoring (Bonczar et al. 2005). Consequently, state transportation agencies rely solely on their past experiences and refinement when constructing integral bridges. This implies a number of limitations on their use; the most notable include bridge length, skew, curvature, foundation types, bridge sites, and provision for approach slabs at both ends of the bridge.

This paper examines the relation between depth of predrilled holes and abutment pile bending stresses using a number of parameters; soil profile, skew, number of spans, and bridge length for the case of a skewed steel integral abutment bridge. In addition, the paper investigates the effects of predrilled holes on pile deflections and on the axial load carrying capacity of piles. End bearing steel H piles oriented with their weak axis perpendicular to the centerline of the bridge are used.

2. Integral Abutment Bridges

Integral abutment bridges are girder bridges with no expansion joints in the bridge deck and no bearings at the abutments. The ends of girders are integral with the abutments; cast into a concrete end diaphragm, which is rigidly connected to a concrete pile cap. The pile cap is supported by a single row of vertical piles (Fig. 1). Pile flexibility accommodates thermal expansion and contraction of the superstructure.

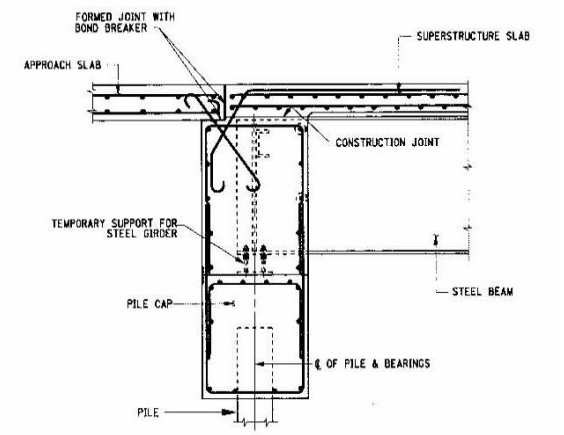

Fig. 1. New York State DOT steel superstructure integral abutment detail

Integral abutment bridges differ from conventional bridges and rigid frame bridges in the manner superstructure movement is accommodated. The superstructure movement is due to temperature changes, creep, and shrinkage and is primarily horizontal translation. An integral abutment bridge accommodates superstructure movement by flexure of the piling and by provision of cycle-control (expansion) joints at the roadway end of the approach slabs. Conventional bridges accommodate superstructure movement by means of deck expansion joints combined with fixed and expansion bearings. Rigid frame bridges accommodate the effects of temperature change, creep, and shrinkage with full height abutment walls that are fixed or pinned at the footing level.

Use of integral abutment bridges offers numerous advantages over conventional bridges. This includes lower construction and maintenance costs (Amde, A.M. and Klinger, J.E. 1988), faster construction, enhanced protection for weathering steel girders (Wasserman and Walker 1996), reduction in the magnitude of impact loads that leads to improved vehicular riding quality (Mistry 2005), enhanced seismic performance (Greimann et al. 1987; Hoppe and Gomez 1996), additional live load capacity to resist potentially damaging overloads (Wasserman and Walker 1996), and lower end span to interior span ratio (Harvey and Kennedy 2002).

Despite their advantages over conventional bridges, there are limitations on the use of integral abutments. The reason for those limitations is to reduce the magnitude of passive earth pressures behind the integral abutments and minimize stresses in the integral abutment piles. The list of limitations aim to reduce the magnitude of passive earth pressures behind the abutments include (1) bridge length to control the amount of backfill compression and consequently the magnitude of passive pressures, (2) abutment height to reduce the magnitude of passive pressures, (3) use of well-graded, free-draining backfill material to control the magnitude of passive pressures, (4) use of approach slab to prevent backfill compaction by the vehicular traffic, and (5) use of moderate skew to shorten the length of abutments exposed to passive pressures. The list of limitations aim to minimize pile stresses include (1) use a single row of vertical slender piles to minimize resistance to longitudinal deck movements, (2) use of predrilled holes around piles in stiff soils, and (3) use of only slight curvature. In addition, there are limitations related to the suitability of the bridge site; this includes adequate depth to bedrock as well as potential for liquefaction and scouring. Furthermore, successful implementation of integral abutment bridges requires attention to construction sequence and good guidance to the contractor in the contract documents (Harvey and Kennedy 2002).

3. Predrilled Holes Around Piles Supporting Integral Abutments

For stiff soil conditions, predrilling oversize holes and surrounding the piles with loose granular soil (Fig. 2) has emerged as an effective method to increase pile flexibility (Dunker and Liu 2007), reduce bending stresses in the piles and increase their vertical load capacity (Yang et al. 1985; Greimann et al. 1986; Greimann and Amde 1988; Crovo 1998; Faraji 1997; Khodair and Hassiotis 2003).

Yang et al. (1985) demonstrated that predrilling holes to replace stiff soils with loose sand greatly increases the vertical load carrying capacity of piles. The predrilled length of the holes was a significant factor. Using HP 250x62 steel piles, 1.8-3 m of length was necessary to take full advantage of predrilling. Mourad and Tabsh (1998) report that the predrilled holes need to be 3-6 m deep, measured from the pile head. Crovo (1998) and Wasserman (2001) report that the depth of the prebored holes should be at least 2.5 m while Mistry (2005) recommends the use of 3 m deep predrilled holes. Table 1 summarizes state DOT practices governing the use of predrilled holes around piles supporting integral abutments.

Table 1. State DOT practices for predrilled holes (Olson et al. 2009)

State	Comments
IA	Predrill to 8 feet for bridges over 130 feet long, and fill the hole with bentonite
IN	Predrill to 8 feet if foundation soil is hard
KS	Not reported
MA	Predrill to 8 feet and fill with loose granular material
ME	Predrill to 10 feet
MI	Predrill to 10 feet
MN	Predrill only in very compact soil to facilitate pile driving rather than to influence IAB behavior
MO	Predrill only in new fill to prevent downdrag on the piles
NE	Predrill to the engineer's recommendation
NJ	Predrill to 8 feet for bridges over 100 feet long
NY	Predrill to 8 feet and fill with loose granular material
OH	Not recommended
OR	Not recommended
SD	Predrill to 10 feet
TN	Not reported
VT	Predrill only in very compact soil
WI	Not reported
WV	Predrill to 15 feet, or predrill to bedrock if rock is between 10 and 15 feet below ground surface

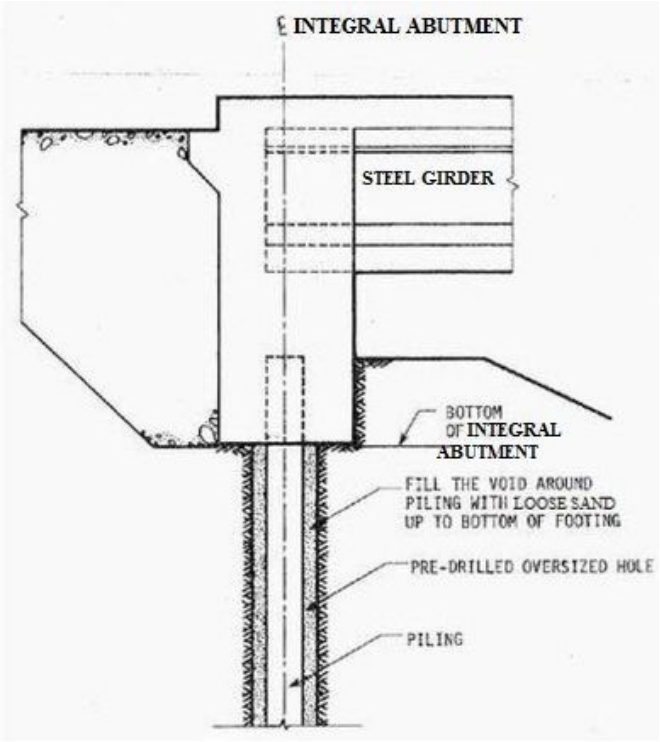

Fig. 2. Predrilled hole detail (Yang et al. 1982)

4. Pile Section Size and Length Considerations

This study is performed using HP 250X62 steel piles oriented with their weak axis perpendicular to the centerline of the bridge (Fig. 3). In practice, however, whenever the HP 250X62 piles have insufficient structural resistance, bigger HP sections are used. This includes HP 250x85, HP 310x110, HP 310x125, HP 360x152, or HP 360x174 sections. The flexibility of the pile sections, regardless of their size is ensured by making the holes twice the diameter of the pile and sufficiently deep (Dunker and Liu 2007). For HP sections, the equivalent diameter of the pile is equal to twice the length of the equivalent radius given by the expression (Fig. 4)

$$R_{equiv.} = (b + h) / \pi$$

where

$R_{equiv.}$ is the equivalent radius of the HP steel section

b is the flange width of the HP steel section

h is the depth of the HP section

π is a mathematical constant that is the ratio of a circle's circumference to its diameter and is equal to 3.14

Although steel H-piles are most frequently used to support integral abutments, cast-in-place concrete piles, prestressed concrete piles, steel pipe piles (open ended or concrete filled), drilled shafts, and spread footings are also used by states.

Use of minimum length of piling is critical for integral abutment bridges. This is due to the fact that the overall length of a pile is relevant to the pile's flexibility and its ability to accommodate abutment movement—the longer the pile, the more flexible is (GangaRao et al. 1996) and the higher is its lateral load carrying capacity (Begum and Muthukkumaran 2008). Consequently, there is a need to ensure that the piles have sufficient flexibility to accommodate the horizontal displacements of the superstructure (Mistry 2005) and that the depth of overburden provides fixed support conditions. This precludes the use of integral abutments where the depth to bedrock is considered shallow, less than 4 m from the ground surface (Hartt et al. 2006) or where piles cannot be driven

through at least 3 to 4.5 m of overburden (Burke 1993; Hoppe and Gomez 1996). Others (Vermont Agency of Transportation Integral Abutment Bridge Design Guidelines) stipulate a minimum pile embedment length of 5 m below the bottom of the pile cap. For instances where one abutment is founded directly on bedrock, but there is sufficient depth for piles to flex at the other abutment, the abutment on bedrock may simply be considered the center of the bridge and piles at the other abutment can be checked for thermal movement based on the entire length of the bridge, rather than half the length (Dunker and Abu-Hawash 2005).

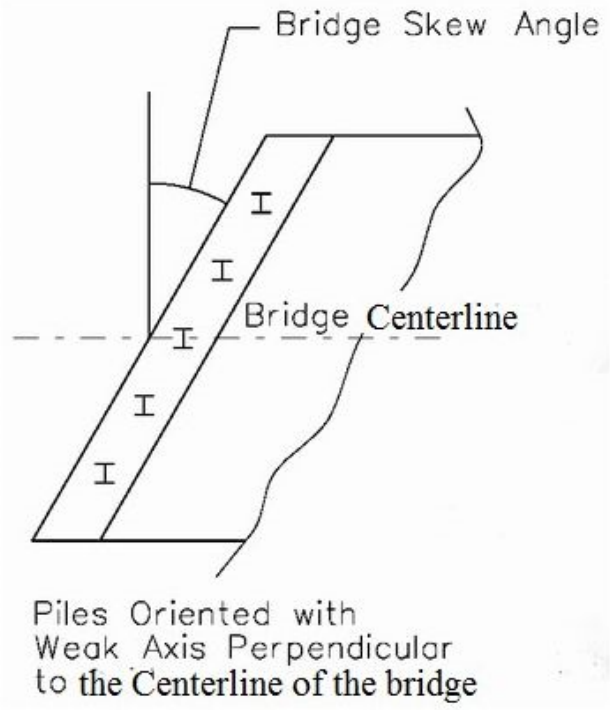

Fig. 3. Pile orientation

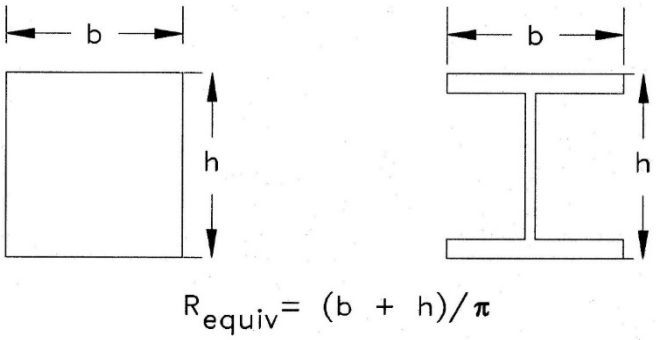

Fig. 4. Equivalent radius of HP section

5. Finite Element Model

A three-dimensional nonlinear finite element model was developed for this parametric study. The model includes the bridge superstructure and substructure as well as the soil behind and below the integral abutments. The model consists of shell elements for the deck slab, girders, and piles; solid elements for the abutments; and nonlinear spring elements for the soil. The study was conducted using the ABAQUS general-purpose nonlinear finite element analysis program. ABAQUS contains an extensive library of elements that can model any geometry. In addition, it has an extensive list of material models that can simulate the behavior of engineering materials including metals and reinforced concrete as well as geotechnical materials such as soils and rock.

The shell element type S4R5 was used to model the deck slab, girders, and piles. The S4R5 shell element is a 4-node doubly-curved thin shell that reduces integration with hourglass control using five degrees of freedom per node, 1, 2, 3 (Δx, Δy, Δz) and two in-surface rotations. The solid element C3D8 was used to model the abutments. The C3D8 element is an 8-node linear brick element with three active degrees of freedom, 1, 2, 3 (Δx, Δy, Δz). The nonlinear spring element SPRING1 was used to simulate the soil behavior. This spring element has six active degrees of freedom, 1, 2, 3, 4, 5, 6 (Δx, Δy, Δz, Θx, Θy, Θz).

The bridge superstructure (Fig. 5) is comprised of a 178 mm thick reinforced concrete slab that sits on six steel girders spaced at 1.83 m. The width of the overhangs on each side is 610 mm. The girders are integrated into the abutments at both ends of the bridge (Fig. 1 and Fig. 9). The abutments are 915 mm wide and have a height of 2.31 m

The deck slab is modeled as shell elements. Nodes are placed at the mid-depth of the reinforced concrete slab at both ends of the bridge superstructure cross section, mid-points between girders, and at the ends and midpoint of girders' top flange

The steel girders are modeled as shell elements with nodes at each end of the flanges and three nodes along the web; two of the web nodes located at the intersection of the web and the flanges. The nodes at the top of each girder are connected to the nodes in the mid-depth of the concrete deck slab using a rigid connection. In addition, the nodes for the concrete deck slab and steel girders are repeated along the bridge length; each node is repeated ten times at equal spaces along the length of each span.

Fig. 6 illustrates the mesh layout along the length of the bridge and the integration between the bridge superstructure and the abutment. It also illustrates the mesh in the abutment cross section; a three-node layer at the top of the abutment, along the slab center line; top, center, and bottom of girders; along top of pile, and at the bottom of the abutment.

The abutments are modeled as solid elements; each element has eight nodes. The nodes are along the same lines in the superstructure and each layer along the abutment cross section

has three nodes; two at the edges and one along the abutment centerline

Piles are modeled as shell elements with the same number of nodes at each layer as the steel girders, that is, seven nodes at each layer (Fig. 7). The pile itself is divided into twenty layers at equal spaces and one layer at the top of the pile. The length of the HP 250X62 steel piles is 12.5 m, where 300 mm is embedded into the abutment and the remaining 12.2 m is driven into the soil, and divided into twenty equally-spaced layers; the length of each layer is 610 mm.

Soil is modeled using nonlinear springs. There are three springs at each node along the length of the pile (Fig. 8). The vertical spring acting in the z-direction represents the friction resistance to the vertical movement of the pile. The other two springs simulate soil resistance to lateral movement in the x and y directions. All three springs are nonlinear and their force-displacement values are calculated using the modified Ramberg-Osgood model. The tip of the end bearing pile sits on rock and represents fixed end boundary conditions.

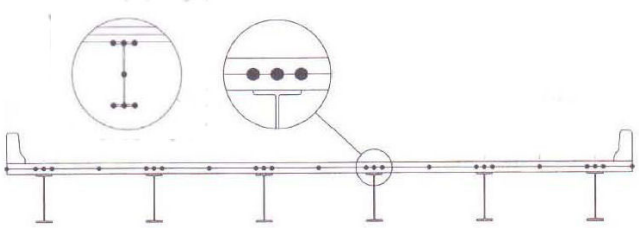

Fig. 5. Bridge superstructure model

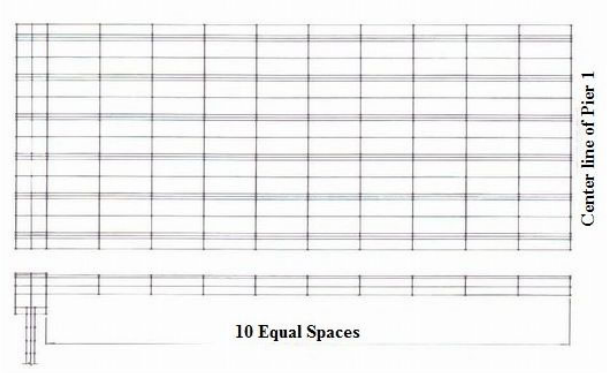

Fig. 6. Plan and elevation view of the mesh layout of the first span of the model

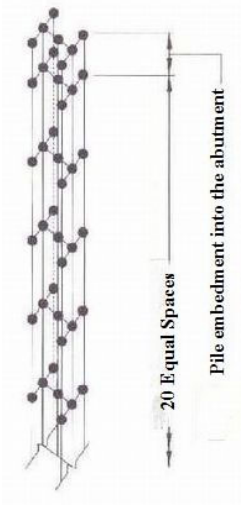

Fig. 7. Layout of nodes in the steel pile

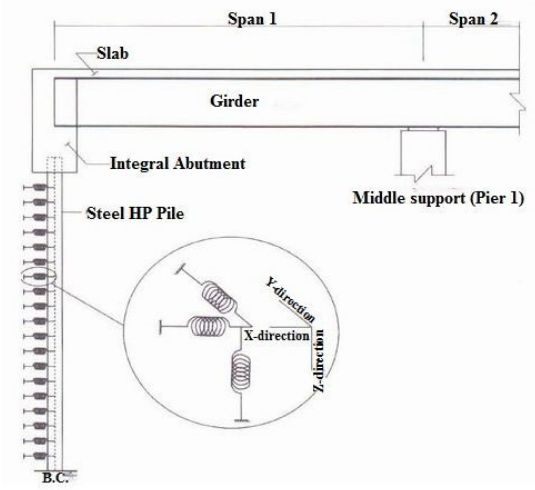

Fig. 8. Soil modeling

6. Soil Profiles

Four depths of predrilling are used in this study (Fig. 9). The first soil profile, S1, consists of only one type of soil; very stiff clay that extends from the bottom of the abutment to the pile tip. The other three soil profiles consist of two types of soil; the top layer is loose sand and represents a pile placed in a predrilled hole filled with loose sand, and the bottom layer is very stiff clay that extends to the pile tip. Fig. 9 indicates the depth of both layers for all four soil profiles S1 to S4. Table 2 describes the soil properties of both types of soil.

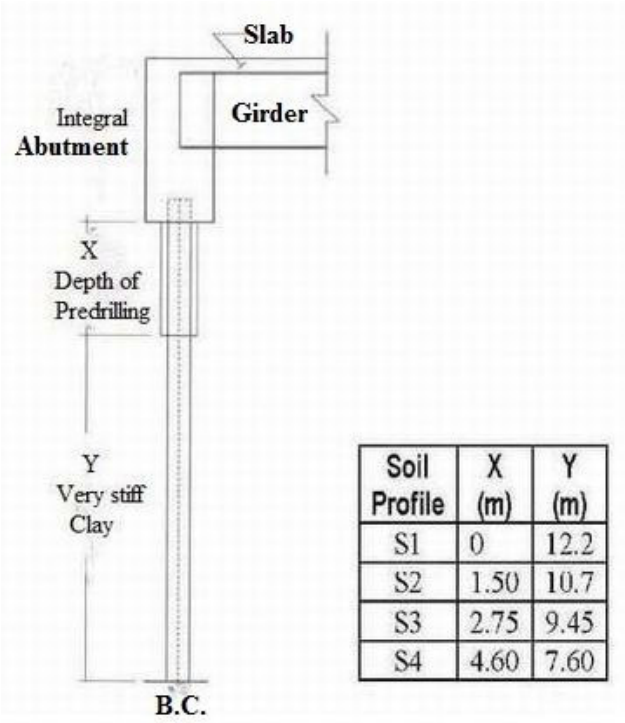

Soil Profile	X (m)	Y (m)
S1	0	12.2
S2	1.50	10.7
S3	2.75	9.45
S4	4.60	7.60

Fig. 9. Layout of the four soil profiles

Table 2. Soil Properties

Loose Sand (Layer X in Fig. 9)	Effective unit soil weight (submerged unit weight) $\gamma = 8.6$ KN/m^3 Angle of internal friction $\Phi = 30^o$
Very Stiff Clay (Layer Y in Fig. 9)	Effective unit soil weight (submerged unit weight) $\gamma = 10.2$ KN/m^3 Undrained cohesion of the clay soil Cu = 239.4 KPa Strain of clay at 50 percent of soil strength $\varepsilon_{50} = 0.005$

7. Pipe-Soil Interaction

According to Greimann et al. (1984), soil characteristics can be described by three types of soil resistance versus displacement curves. The first characteristic is represented by a p-y curve (Fig. 10), which describes the relationship between the horizontal resistance (horizontal force per unit length of pile) of the soil at a depth z along the pile length and the corresponding horizontal displacement of the pile at that depth. The second characteristic is represented by an f-z curve, which describes the relationship between the vertical skin frictional resistance (vertical force per unit length of pile) of the soil at depth z along the pile length and the relative vertical displacement between the pile and the soil at that depth. The third characteristic is represented by a q-z curve, which describes the relationship between the bearing resistance (vertical force on the effective, pile-tip area) at the pile tip and the vertical settlement of the pile tip. All three types of curves assume nonlinear soil behavior.

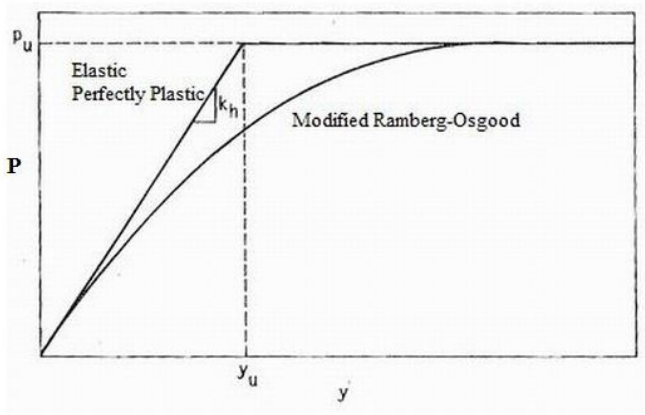

Fig. 10. Modified Ramberg-Osgood P-y curve (Amde et al. 1987)

8. Modified Ramberg Osgood Model

Research conducted by Amde et al (1982), Greimann et al (1984), Greimann and Amde (1988) utilized an idealized model based on the modified Ramberg-Osgood model to approximate the load-displacement curves for the modeling of the nonlinear pile-soil interaction. The parameters needed for the model are calculated from the soil and pile properties. The modified Ramberg-Osgood model is used to approximate all three types of load-displacement curves.

The modified Ramberg-Osgood P-y curve is expressed mathematically using the equation

$$p = \frac{k_h y}{\left[1 + \left[\frac{y}{y_u}\right]^n\right]^{1/n}}$$

$$y_u = \frac{p_u}{k_h}$$

where

k_h is the initial lateral stiffness of the soil

p is the lateral soil resistance

p_u is the ultimate lateral soil resistance at depth z along the pile length

n is a dimensionless shape parameter. The effect of the shape parameter on the modified Ramberg-Osgood equation is shown in Fig. 11

y is the lateral displacement of the pile

y_u is the lateral displacement of the pile in inches that is associated with an elastic- plastic soil material when the resistance p equals the resistance p_u

Fig. 10 presents a comparison between the modified Ramberg-Osgood curve and a typical *p-y* curve. The figure shows that the typical *p-y* curve simplifies the nonlinear soil

behavior with the use of an elastoplastic curve. This curve has two parts: (1) elastic portion, which is defined with a slope equal to the secant soil modulus for the case of clay, and initial soil modulus for the case of sand, and (2) plastic portion, which is the ultimate soil resistance per unit length of pile, p_u.

Fig. 11 presents a non-dimensional form of the modified Ramberg-Osgood *P-y* equation in terms of p/p_u versus y/y_u. The graph clearly indicates the effect of shape parameter n in the modified Ramberg-Osgood *P-y* equation.

9. Effect of Skew Angle and Depth of Predrilled Holes on Maximum Pile Bending Stresses

All four soil profiles S1 to S4 (Fig. 9) were analyzed for temperature load using a temperature variation of 90□F and five skew angles (0º, 15º, 30º, 45º, and 60º). The results of the analyses are shown in Table 3. The models used in the finite element analyses comprised of four equal spans of 30.5 meters. Piles were oriented with their weak axis perpendicular to the centerline of the bridge regardless of the skew angle. In addition, piles were assumed perfectly elastic to eliminate any possibility of plastic hinge formation.

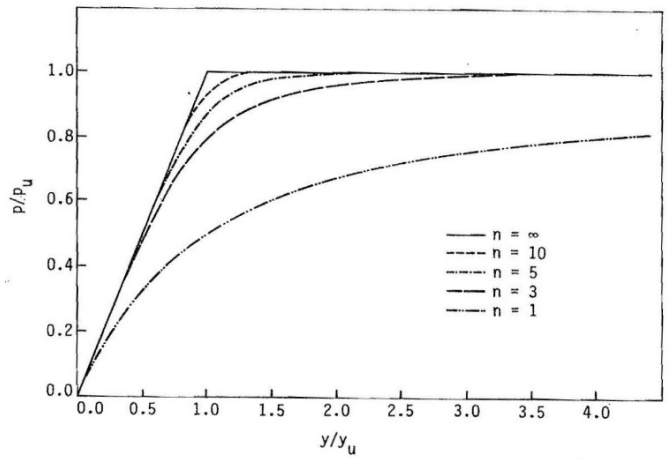

Fig. 11. Non-dimensional form of the modified Ramberg-Osgood P-y equation (Amde et al. 1987)

The results tabulated in Table 3 are plotted in Figs. 12 and 13, which indicate higher pile bending stresses with increasing skew angle (Fig. 12), but reduced pile bending stresses with increasing depth of predrilled holes (Fig. 13). The graph in Fig. 13 indicates a significant reduction in pile stresses when the depth of predrilled holes reaches 2.75 m. Further reductions in pile stresses are shown for predrilled depths exceeding 2.75 m; however, the reduction in pile stresses for depths exceeding 2.75 m is small in percentage terms compared to pile stress reductions for depths up to 2.75 meters.

Fig. 13 indicates that the skew angle impacts the effectiveness of predrilling holes. This can be explained by the fact that at larger skew angles the length of abutment exposed to passive pressures increases from width W to W/cosΦ where Φ is the skew angle.

In order to confirm that 2.75 m is an effective depth for predrilled holes in integral abutment bridges, another set of models having a 2.15 m deep predrilled holes was analyzed. The results indicate that the reduction in pile stresses due to 2.15 m deep predrilled holes exceed the reduction in pile stresses produced by soil profile S2, that is, 1.5 m deep predrilled holes, but is less than the reduction in pile stresses produced by soil profile S3, that is, 2.75 m deep predrilled holes. This is shown in Figs. 14 and 15. Fig. 14 illustrates the percent reduction of pile stresses versus depth of predrilled holes for varying skew angles and Fig. 15 illustrates the percent reduction of pile stresses versus skew angle for varying depth of predrilled holes.

Table 3. Maximum pile stresses in soil profiles S1 thru S4 for varying skew angles

Skew Angle	Pile Stresses (MPa) for Soil Profile			
	S1	S2	S3	S4
0º	398	376	301	287
15º	401	385	309	295
30º	406	392	317	302
45º	414	403	330	316
60º	424	417	359	346

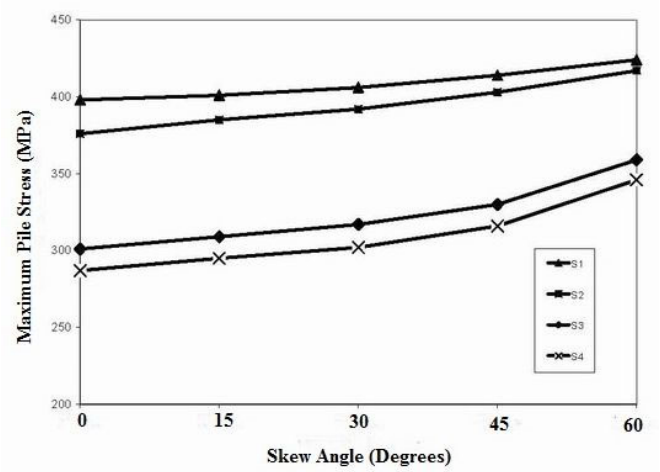

Fig. 12. Maximum pile stresses versus skew angle for different soil profiles

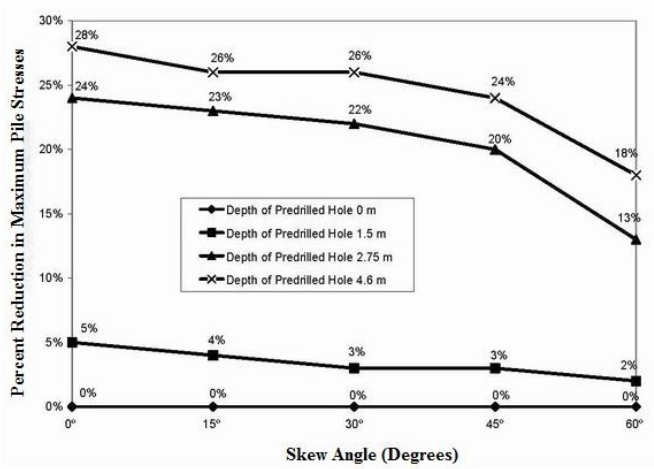

Fig. 13. Reduction in maximum pile stresses versus skew angle for varying depth of predrilled holes

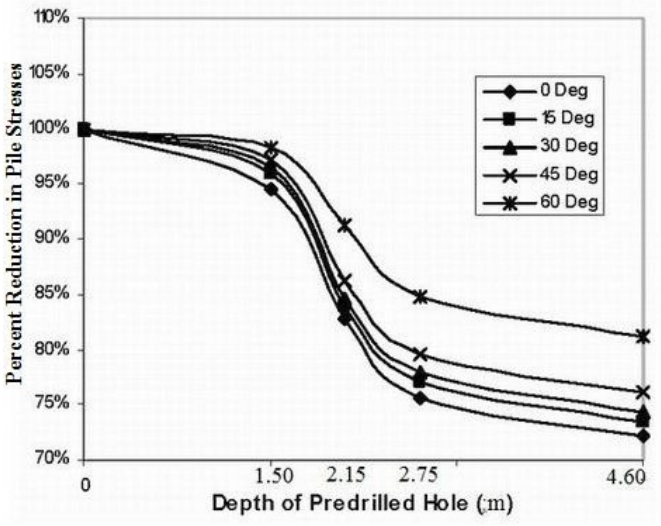

Fig. 14. Percent reduction in pile stresses versus depth of predrilled holes for varying skew angles

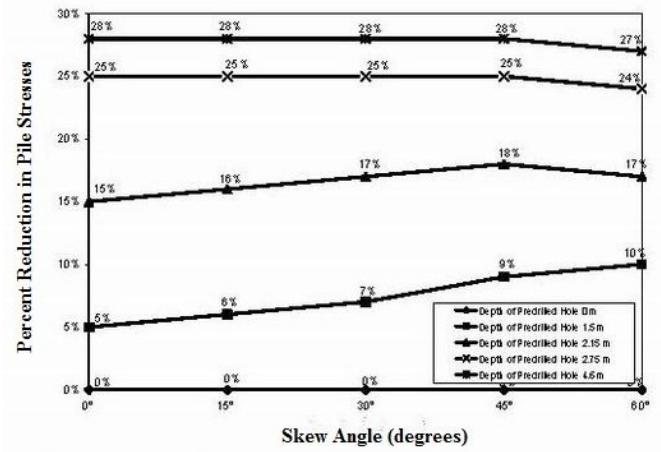

Fig. 15. Percent reduction in pile stresses versus skew angle for varying depth of predrilled holes

10. Effect of Predrilled Holes on Pile Deflections and Pile Axial Load Carrying Capacity

To study the effect of predrilled holes on pile deflections, two different soil profiles were used: (1) the very stiff clay profile (S1), and (2) the soil profile with 2.75 m deep predrilled hole filled with loose sand (S4). The deflected shapes (Fig. 16) indicated that in the very stiff clay profile (S1), the point of fixity was about 3.35 to 4 m below the bottom of the abutment, while for piles driven in very stiff clay with 2.75 m deep predrilled hole filled with loose sand at the top (S4), the point of fixity was about 4 to 4.9 m below the bottom of the abutment. The models used were for an 8-span bridge consisting of eight 30.5 m long spans, for a total bridge length of 244 m at a skew angle of 60º.

There is a significance in the fact that the depth of the point of fixity is higher in piles without predrilled holes compared to piles with predrilled holes. This is like analyzing a short cantilever column with an axial load applied at its top and subject to a lateral movement compared to analyzing a longer column subject to the same loading conditions as the short one. The short column will fail under a lower axial force than the long column for the same amount of lateral deflection. This is shown in Fig. 17, which indicates that piles with 2.75 m deep predrilled hole filled with loose sand (S4) have a higher vertical load carrying capacity compared to piles in very stiff clay profile (S1) for the same amount of lateral displacement.

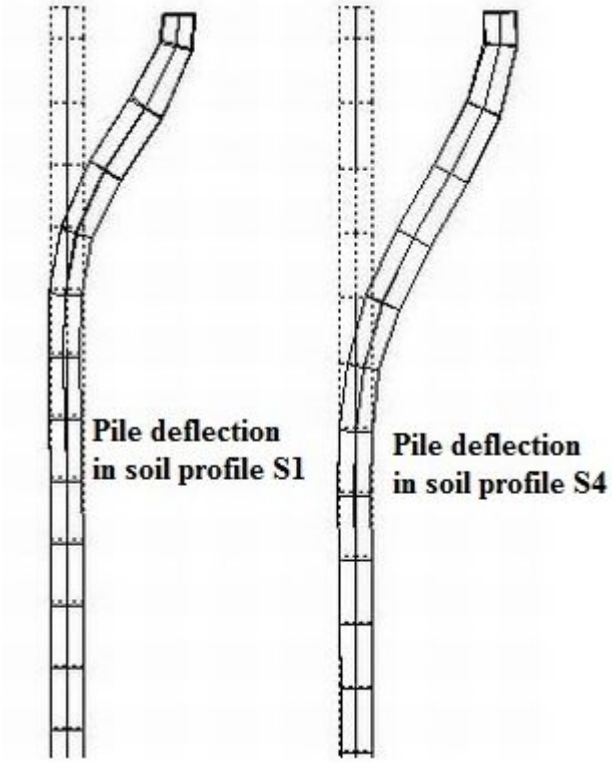

Fig. 16. Effect of predrilled holes on pile deflections

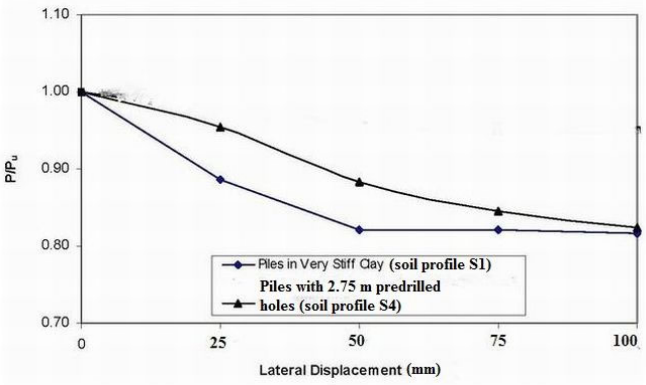

Fig. 17. Axial load carrying capacity of piles versus lateral displacement

11. Effect of Number of Spans on Maximum Pile Bending Stresses

To study the effect of number of spans on the maximum stresses in the piles, two models for 61 m long bridges were analyzed using a different number of spans. The first model consisted of two 30.5 m long spans, while the second model consisted of four 30.5 m long spans. Both models were analyzed using the three-dimensional finite element model described earlier using various skew angles. This investigation used two different soil profiles; the very stiff clay profile (S1) and the soil profile with 2.75 m deep predrilled hole filled with loose sand (S4). The results from both analyses are shown in Table 4. The results indicate a reduction in maximum pile stresses of the order of 30 percent when the number of spans increases from 2 to 4 for both soil profiles.

Table 4. Effect of number of spans on maximum pile bending stresses (MPa)

No. Spans	2	4	2	4
Predrilled Hole	No	No	Yes (2.75 m)	Yes (2.75 m)
0° Skew	343	203	233	144
15° Skew	348	209	239	147
30° Skew	354	217	244	153
45° Skew	368	230	258	163
60° Skew	396	247	287	181

12. Effect of Bridge Length on Maximum Pile Bending Stresses

Four different models were used to investigate the effect of bridge length on maximum piles stresses. The models had different bridge lengths; 61 m, 122 m, 244 m, and 366 m. Each model was analyzed using five different skew angles, that is, 0, 15, 30, 45, and 60 degrees in two soil profiles; the very stiff clay profile (S1) and the very stiff clay with 2.75 m deep predrilled hole filled with loose sand (S4). The results, which are shown in Figs. 18 and 19 show the pile stresses as a percentage of the pile stresses in the piles of the 366 m long bridges at 60-degree skew.

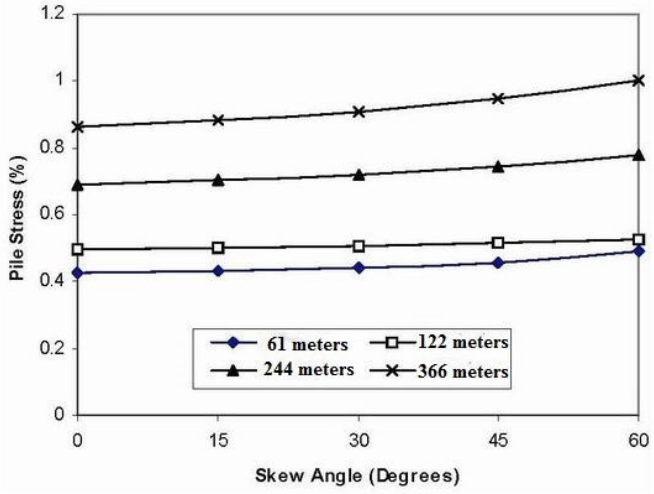

Fig. 18. Effect of bridge length on maximum pile stresses in soil profile S1

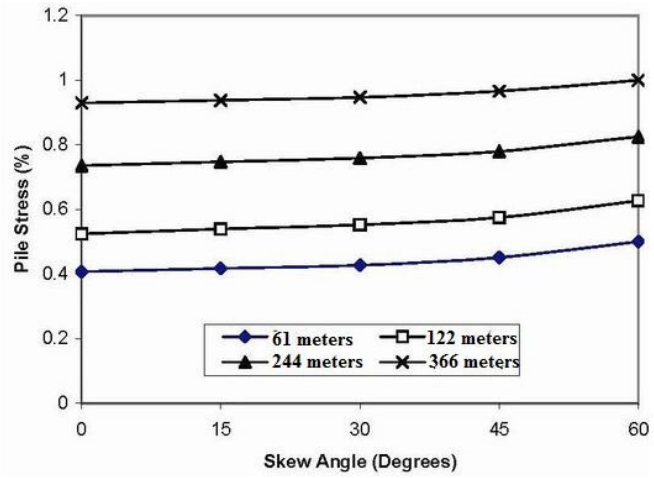

Fig. 19. Effect of bridge length on maximum pile stresses in soil profile S4

13. Conclusions

The results of this study point out to a number of observations related to the behavior of skew integral abutment bridges. This includes the following: (1) increased bridge length and skew angle induces higher bending stresses in the piles supporting the integral abutments, (2) increased number of spans and use of predrilled holes around the piles of integral abutments results in reduced pile bending stresses, and (3) use of predrilled holes increases the vertical pile load carrying capacity.

Consequently, use of predrilled holes around piles provides the benefits of reduced pile bending stresses and increased pile vertical load carrying capacity. The results of the analysis also indicate that predrilling to a depth of 2.75 m from the bottom of

the integral abutment provides almost 100 percent of those benefits. In fact, the results indicate that predrilling to a depth of more than 2.75 m yields marginal additional benefits in terms of reduced pile bending stresses and higher vertical capacity in the piles. This is attributed to the fact that most of the horizontal deflections and the largest bending moments occur within the top 2.75 to 3 m of pile length. Consequently, the surrounding soil in this region controls the behavior of the pile, regardless of the type of soil present below this depth.

In conclusion, the results of the analysis suggest that the use of predrilled holes filled with loose sand around the piles of skew integral abutment bridges is an effective method to reduce bending stresses in the piles and increase their vertical load carrying capacity. The depth of predrilled holes is 2.75 m measured from the bottom of the integral abutment.

References

Amde, A.M., Greimann, L.F., and Yang, P.S. (1982). "Nonlinear Pile Behavior in Integral Abutment Bridges," Iowa State University, Ames, IA

Amde, A.M., Klinger, J.E., Mafi, M., Albrecht, P., White, J., and Buresli, M. (June 1987). "Performance and Design of Jointless Bridges," Contract No. DTFH61-85-C-00092, Department of Civil Engineering, University of Maryland, College Park, MD

Amde, A. M., Klinger, J. E., and White, E. J. (1988). "Performance of Jointless Bridges." Journal of Performance of Constructed Facilities, ASCE, Vol. 2, No. 2, May, pp. 111-125

Begum, N.A., and Muthukkumaran, K. (2008). "Numerical Modeling for Laterally Loaded Piles on a Sloping Ground." *12th International Conference of International Association for Computer Methods and Advances in Geomechanics (IACMAG)*, Goa, India

Bonczar, C., Civjan, S., Brena, S., and DeJong, J. (June 2005). "Behavior of Integral Abutment Bridges: Field Data and Computer Modeling," Report No. SPRII.03.20, Department of Civil and Environmental Engineering, University of Massachusetts at Amherst, Amherst, MA

Burke, M.P. (1993). "Integral Bridges: Attributes and Limitations," *Transportation Research Record*, No. 1393, pp. 1-8

Crovo, D. S. (April 1998). "The Massachusetts Experience with Jointless Abutment Bridges." *15th Annual International Bridge Conference*, Pittsburgh, Pennsylvania

Dunker, K. F., and Abu-Hawash, A. (August 2005). "Expanding the Use of Integral Abutments in Iowa," *Proceedings Mid-Continent Transportation Research Symposium*, Ames, IA

Dunker, K., and Liu, D. (2007). "Foundations for Integral Abutment Bridges." *ASCE Practice Periodical on Structural Design and Construction*, Vol. 12, No. 1, pp. 22-30

Faraji, S. (1997). "Behavior of Integral Abutment Bridges in Massachusetts." Project UMTC-96-5, Massachusetts Highway Department, Boston, MA

GangaRao, H., Thippeswamy, H., Dickson, B., and Franco, J. (1996). "Survey and Design of Integral Abutment Bridges," Workshop on Integral Abutment Bridges, Pittsburgh, PA

Greimann, L.F., Yang, P.S., Edmunds, S.K., and Amde, A.M. (August 1984). "Final Report, Design of Piles for Integral Abutment Bridges." Engineering Research Institute, Department of Civil Engineering, Iowa State University; Ames, IA

Greimann, L.F., Amde, A.M., and Yang, P.S. (1986). "Nonlinear analysis of integral abutment bridges." *ASCE Journal of Structural Engineering*, No. 112, pp. 2263 – 2280

Greimann, L.F., Abendroth, R.E., Johnson, D.E., and Ebner, P.B. (1987). "Pile design and tests for integral abutment bridges," Final Report, Iowa Department of Transportation Project HR-273

Greimann, L., and Amde, A. M. (1988). "Design Model for Piles in Jointless Bridges," *ASCE Journal of Structural Engineering*, Vol. 114, No. 6, pp. 1354-1371

Hartt, S.L., Sanford, T.C., and David, W.G. (August 2006). "Monitoring a pile- supported integral abutment bridge at a site with shallow bedrock. Phase II," Report No. ME 01-7, University of Maine; Orono, ME

Harvey, D.I., and Kennedy, D.W. (July 2002) "Integral Abutment Bridges-Design and Constructibility," *6th International Conference on Short and Medium Span Bridges*, Vancouver, Canada

Hoppe, E.J., and Gomez, J.P. (1996). "Field Study of an Integral Backwall Bridge," Report VTRC 97-R7, Virginia Transportation Research Council, Charlottesville, VA

Khodair, Y., and Hassiotis, S. (July 16-18, 2003). "Analysis of Pile Soil Interaction," *ASCE 16th Engineering Mechanics Conference*, University of Washington, Seattle, WA

Mistry, V. (March 16-18, 2005). "Integral Abutment and Jointless Bridges," *FHWA Integral Abutment Jointless Bridges Conference*, Baltimore, MD

Mourad, S., and Tabsh, S. W. (1998). "Pile forces in integral abutment bridges subjected to truck loads," *Transportation Research Record*, No. 1633, pp. 77-83

NYSDOT, *Bridge Design (BD) Sheets*, 2010 (New York State Department of Transportation: Albany, NY)

Olson, S.M., Long, J.H., Hansen, J.R., Renekis, D., and LaFave, J.M. (2009) "Modifications of IDOT Integral Abutment Design Limitations and Details," Report No. FHWA-ICT--09-054, University of Illinois at Urbana-Champaign, Urbana, IL

Vermont Agency of Transportation (VTrans), *Integral Abutment Bridge Design Guidelines*, Second edition, October 2008, Montpelier, VT

Wasserman, E. P., and Walker, J. H. (1996). "Integral Abutments for Steel Bridges." American Iron and Steel Institute, Vol. II, Chap. 5, Highway Structures Design Handbook.

Wasserman, E.P. (May 2001). "Design of integral abutments for jointless bridges." *Structure Magazine*, pp. 24–33

Yang, P.S., Amde, A.M., and Greimann, L.F. (1982), "Nonlinear Finite Element Study of Piles in Integral Abutment Bridges Part 2," Final Report, Iowa Department of Transportation Project HR-273

Yang, P.S., Amde, A.M., and Greimann, L.F. (1985), "Effects of predrilling and layered soils on piles." ASCE *Journal of Geotechnical Engineering*, No.111, pp. 18–31